

Kinetics of Hydrogen Production upon Reduction of Aqueous TiO₂ Nanoparticles Catalyzed by Pd⁰, Pt⁰, or Au⁰ Coatings and an Unusual Hydrogen Abstraction; Steady State and Pulse Radiolysis Study

David Behar* and Joseph Rabani*

Department of Physical Chemistry and Accelerator Unit, The Hebrew University of Jerusalem, Jerusalem 91904, Israel

Received: February 15, 2006; In Final Form: March 16, 2006

Reduction of H⁺ by TiO₂ electrons ($e_{\text{TiO}_2}^-$) in aqueous colloidal solution takes place in the presence of surface metal catalysts. The catalytic reduction gives rise to adsorbed hydrogen atoms. In the presence of Pd⁰ or Pt⁰, material balance shows that most of the adsorbed H atoms combine to molecular hydrogen. When the TiO₂ nanoparticles are partially coated with Au⁰ instead of Pd⁰ or Pt⁰, a higher than expected molecular hydrogen level is observed, attributed to a short chain reaction involving hydrogen abstraction from 2-propanol. This unusual hydrogen abstraction reaction has not been reported before. The mechanism and energy balance are discussed. The surface modification of TiO₂ nanoparticles was carried out by reduction of K₂PdCl₄, H₂PtCl₆, or HAuCl₄ with $e_{\text{TiO}_2}^-$. The latter had been generated through electron injection from hydrated electrons, hydrogen atoms, or 2-propanol radicals, produced by γ or pulse radiolysis prior to the addition of the metal compounds. Upon addition of the metal compounds, immediate reactions take place producing metals clusters (M⁰) by multistep reductions reactions on the TiO₂ surface. The chemical kinetics involving the different metals and the reaction rate constant of e_{aq}^- and $e_{\text{TiO}_2}^-$ with AuCl₄⁻ is also reported.

Introduction

Nobel metal particles deposited on nanocrystallite semiconductors have been used widely to enhance the photocatalytic efficiencies,^{1–6} particularly Pt⁰, Au⁰, or Pd⁰ on TiO₂. The noble metals act as an electron sink promoting interfacial charge-transfer processes in the composite systems.^{7,8} Graetzel⁹ has noted that free diffusion of charge carriers permits electron transfer within a time of 0.1 ps, thus competing effectively with electron–hole recombination. Wang, Heller, and Gerischer¹⁰ have shown that catalyzed oxygen reduction by $e_{\text{TiO}_2}^-$ involving surface metal increases the photocatalytic oxidation yields by preventing accumulation of electrons on the TiO₂ particles, thus inhibiting the rate of electron–hole recombination. Subramanian et al.¹¹ observed a relationship between the photocatalytic activity of TiO₂ film doped with Au⁰ nanoparticles and the effect of gold particle size on the Fermi level of the composite: A greater shift in the Fermi level toward more negative potentials was observed with smaller Au nanoparticles, causing greater photocatalytic reduction efficiency. It has been shown recently (in the ZnO/Pt nanocrystallites, which have energy properties similar to those of TiO₂/Pt), that excess electrons reside exclusively on the Pt⁰.¹² Thus, it is not surprising that the TiO₂/Pt and similar systems show enhanced photocatalytic oxidation such as biphenol, ammonia, and CO compared to bare TiO₂.^{13–16}

A number of works have been published concerning photochemical generation of hydrogen in a Pt⁰ modified TiO₂ surface.^{17,18} Bamwenda et al.¹⁷ studied photocatalytic H₂ generation by Au/TiO₂ and Pt/TiO₂ in illuminated aqueous 5 M C₂H₅-OH suspension and reported strong dependence of the catalytic activity on the preparation method. It has been reported that

the overall activity of Au⁰ was generally about 30% lower compared to Pt⁰. The H₂ yield depended on the metal content, with a maximum in the range 0.3–1 wt % Pt⁰. The yield was found to depend on initial pH (maximum at 4–7) and decreased considerably at highly acidic and highly basic suspensions.¹⁷ Kanno et al.¹⁹ reported that the catalytic activity of Pt/TiO₂ was three times higher than that of Au/TiO₂. Surface Pd⁰ increased the quantum efficiency of the photooxidation of aqueous 2,2-dichloropropionate threefold at 0.01 wt % Pd compared to bare TiO₂.¹⁰ Xu et al.²⁰ studied Pd sputtering on a TiO₂ surface at room temperature and observed competition between Pd⁰ cluster growth and nucleation of new sites. Initially new seeds were formed, but with increasing the amount of deposition manyfold most of the Pd atoms accumulate at the initially produced seeds and only a small portion form new seeds. It was also found that Pd atoms tend to form dimers and tetramers. No isolated Pd atoms were ever observed, suggesting that the dimmer is the smallest stable nuclei.

Reduction reactions of excess electrons in TiO₂ nanocrystallites produced by pulse radiolysis have been studied earlier.²¹ Reduction rates of several substrates were found to depend on TiO₂ particle size. Cu²⁺, ClO₂⁻, ClO₃⁻, NO₂⁻, and NO₃⁻ showed decay of the $e_{\text{TiO}_2}^-$ electron predominately by a single pseudo first-order process. Alternatively, hydrogen peroxide and oxygen show a multiexponential decay. In a recent publication²² we studied the reactions of $e_{\text{TiO}_2}^-$ with H⁺ and water in the TiO₂/Pt system and elucidated the reaction mechanism and radiation yields of H₂. The decay of the TiO₂ electron was found to be a single pseudo first-order process depending linearly on Pt⁰ and H⁺ concentrations. The energy of $e_{\text{TiO}_2}^-$ is not sufficient for generation of free hydrogen atoms, although adsorbed atoms on the Pt⁰ surface are produced. These atoms eventually combine to molecular hydrogen. It has been shown that the energy of

* Corresponding authors. E-mail: behar@vms.huji.ac.il; rabani@vms.huji.ac.il.

the adsorbed hydrogen atom on the Pt^0 surface is not sufficient to abstract hydrogen from 2-propanol. A similar observation was reported in Au/TiO_2 by Hussein and Rudham.²³

The purpose of the present work is to expand the earlier work to additional metals, namely Pd^0 and Au^0 , comparing their reactivity toward H^+ and H_2O reduction and their catalytic role in adsorbed hydrogen atom reaction.

Experimental Section

Colloidal TiO_2 solutions were prepared by hydrolysis of TiCl_4 (Aldrich 99.9%). As reported previously,²⁴ 25 mL of TiCl_4 was introduced very slowly under a stream of argon and vigorous stirring into 700 mL of 0.1 M HCl solution cooled at 0 to 4 °C. Thirty minutes after the addition of the TiCl_4 , the solution was dialyzed against HCl solution at pH 3 (pore size cutoff 6000–8000). The suspension was kept at 45 °C for several days to increase the size of the particles to an average diameter of about 5 nm. TiO_2 concentrations, in terms of molecules, were determined by spectrophotometric measurements at 215 nm using $\epsilon = 6050 \text{ M}^{-1} \text{ cm}^{-1}$.

Radiolysis. A ^{137}Cs γ source of 9 Gy/min or a linear electron beam accelerator (Varian 7715) operated at 5 MeV and maximum current of 200 mA with 1.5 μs pulse duration were used as the radiation sources for production of excess electrons in the TiO_2 nanoparticles. At the highest electron beam intensity about $1.5 \times 10^{-5} \text{ M}$ reducing radicals were produced by a single pulse (taking $\text{Ge}_{\text{aq}}^- + \text{G}(\text{OH}^\bullet) + \text{G}(\text{H}^\bullet) = 6$, where G_x stands for the number of X molecules produced by 100 eV absorbed radiation). The absorbance changes of $\text{e}_{\text{TiO}_2}^-$ were monitored at 600 nm. The reactivity of Au^{3+} , Pd^{2+} , and Pt^{4+} toward the hydrated electron, e_{aq}^- , was studied by its decay kinetics using pulse radiolysis by competition with methyl viologen (MV^{2+}) applying 0.2 μs pulses, which yields about $1 \times 10^{-6} \text{ M}$ e_{aq}^- per pulse. The absorption changes of the methyl viologen radical were also followed at 600 nm.

TiO_2 Coatings with Pt, Au, and Pd. Deaerated (Ar bubbling) colloid solutions of TiO_2 (4–5 mL of 0.2M) containing (0.2–2) M 2-propanol, sealed in test tube by means of a rubber septum were irradiated by γ rays or electron beam. Under these conditions $\text{e}_{\text{TiO}_2}^-$ builds up; its concentration was adjusted to exceed by about 30% the equivalent concentration of the metal precursor (namely $[\text{e}_{\text{TiO}_2}^-] = 1.3 \times 2x[\text{Pd}(\text{II})]$ or $1.3 \times 3x[\text{Au}(\text{III})]$ or $1.3 \times 4x[\text{Pt}(\text{IV})]$). In the absence of the metal salts $\text{e}_{\text{TiO}_2}^-$ is stable for weeks. Upon injection of the metal complexes, instantaneous reduction to the free metals is observed. The unreacted electrons remaining at the end of the reduction process were destroyed by saturating the solution with oxygen. Finally the oxygen was removed by saturating again with argon.

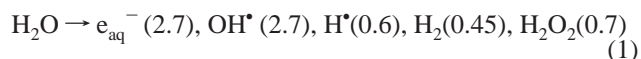
Kinetic Measurements. Pulse radiolysis experiments were carried out in a 2 cm quartz cell (6 cm light path) at (22 ± 2) °C. The pulse duration was 0.2–1.5 μs , yielding $(1-7) \times 10^{-6} \text{ M}$ e_{aq}^- . Dosimetry was carried out by measuring the 480 nm absorption of $(\text{SCN})_2^{\bullet-}$ produced in 5 mM N_2O saturated SCN^- solution at neutral pH, using $\epsilon_{(\text{SCN})_2^{\bullet-}} = 7600 \text{ M}^{-1} \text{ cm}^{-1}$. The kinetics of e_{aq}^- reaction with methyl viologen and of $\text{e}_{\text{TiO}_2}^-$ reaction with the metal complexes was studied by the 600 nm absorbance changes. Rate constants of the reaction of e_{aq}^- with the metal complexes were determined by competition with methyl viologen. For kinetic measurement of $\text{e}_{\text{TiO}_2}^-$ reactions with H^+ and water, which endure several hours, solutions of TiO_2 colloid coated with the reduced metals were transferred into a quartz cell and bubbled with argon for at least 20 min. The 1 cm cell was subsequently irradiated by electron beam,

receiving 30–40 consecutive pulses of about 30 Gy each within several seconds. The TiO_2 nanoparticles in the suspension become loaded with excess $\text{e}_{\text{TiO}_2}^-$. The cell was then transferred to a Hewlett-Packard diode array spectrophotometer at 25 °C for the kinetic measurements. The optical density was monitored against air without compensating for the cells reflection and absorbance, which in some cases, stable coloration of the quartz during irradiation took place.

Hydrogen Determination. Several (2–3) sealed test tubes containing Ar-saturated colloid solutions of TiO_2/M^0 in the presence of 2-propanol were irradiated in a ^{137}Cs γ source for 3 h, receiving a total dose of 1.6 kGy. The irradiation was carried out together with the same number of reference samples containing aqueous 2-propanol (0.2 M or 2 M) in the absence of TiO_2/M^0 at acid pH. The reference samples served to determine the hydrogen yields by comparison between the hydrogen signals in the reference and in the TiO_2/M^0 solutions. The test tubes were left at room temperature for 17–20 h to ensure completion of the reaction producing hydrogen. During measurements the test tubes were kept in a 25 °C thermostat. Given volumes from the gas phase, equilibrated by vigorous shaking of the samples were injected to the HP-5890 gas chromatograph (TCD detector, Porapak column from Supelco and argon as the gas carrier).

Results and Discussion

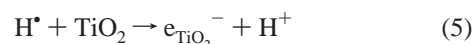
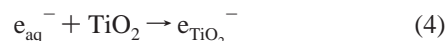
The primary radicals and molecules produced in water upon electron-beam or γ irradiation are shown in eq 1. The numbers in parentheses represent the respective G values. Where G stands for the number of radicals or molecules produced per 100 eV of absorbed radiation.



In the presence of 2-propanol the OH^\bullet and H^\bullet radicals abstract hydrogen from the alcohol to produce the 2-propanol radical $(\text{CH}_3)_2\text{C}^\bullet\text{OH}$ as shown in reactions 2 and 3.



In the absence of oxygen and the metal complexes the reducing radicals react with TiO_2 nanoparticles to produce the stable $\text{e}_{\text{TiO}_2}^-$ radical (reactions (4–6)).



Pulse Radiolysis Experiments. Reaction of e_{aq}^- with the Noble Metal Complexes. The reaction of hydrated electrons with PtCl_6^{2-} and PdCl_4^{2-} have been reported previously.²⁵ We have verified the above rate constants and determined the e_{aq}^- rate constants with AuCl_4^- by competition of the metal complexes with methyl viologen. Ar-saturated 0.2 M *tert*-butyl alcohol solutions containing $2 \times 10^{-5} \text{ M}$ methyl viologen at pH 5.5 were exposed to pulses of 0.2 μs duration ($1 \times 10^{-6} \text{ M}$ e_{aq}^-). The *tert*-butyl alcohol was chosen to scavenge the OH^\bullet radicals (reaction 7) because its relatively inert radical intermediate cannot interfere with the studied competition reactions. Under

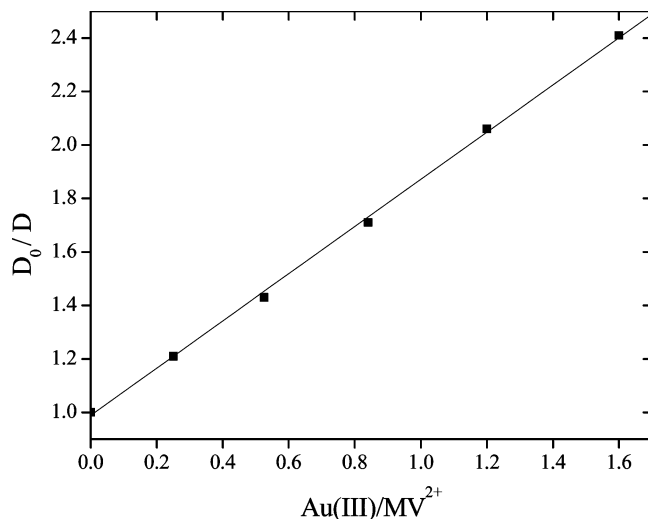
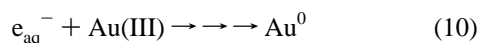
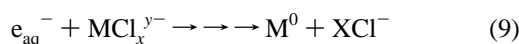
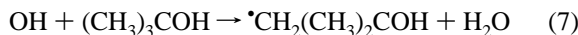


Figure 1. Competition of AuCl_4^- and MV^{2+} for e_{aq}^- [MV^{2+}] = 2×10^{-5} M, 3 mM buffer acetate pH 5.5, Ar-saturated, 0.2 M *tert*-butyl alcohol, 0.2 μs pulse ($1 \mu\text{M } e_{\text{aq}}^-$). Absorption of $\text{MV}^{\bullet+}$ was followed at 600 nm.

the conditions of this work, at pH 5.5 about 6.5% of the reducing radicals are in the form of H atoms and the rest 93.5% are solvated electrons, e_{aq}^- . Reactions of hydrogen atoms are shared between *tert*-butyl alcohol, MV^{2+} , and the respective metal complexes; therefore, the relative concentration of the H atoms is small and does not interfere with the competition reactions measured here. The hydrated electron, e_{aq}^- , reduces methyl viologen according to reaction 8 with an average rate constant $k_8 = 6.9 \times 10^{10} \text{ M}^{-1}\text{sec}^{-1}$.²⁵



The expression describing the competition reactions of a metal complex and MV^{2+} (reaction 8 and 9) is $D_0/D = k_9[\text{MCl}_x^{y-}]/k_8[\text{MV}^{2+}] + 1$, where D_0 is the maximum optical density of the $\text{MV}^{\bullet+}$ radical in the absence of MCl_x^{y-} and D is the maximum optical density of $\text{MV}^{\bullet+}$ in the presence of MCl_x^{y-} . From plots of D_0/D versus $[\text{Pd(II)}]/[\text{MV}^{2+}]$ and $\text{Pt(IV)}/\text{MV}^{2+}$ (not given here) we obtained $k_{9\text{Pd}} = 1.2 \times 10^{10}$ and $k_{9\text{Pt}} = 1.9 \times 10^{10} \text{ M}^{-1}\text{s}^{-1}$ in very good agreement with the value published previously.²⁵ Figure 1 presents the competition plot for Au(III) from which a rate constant $k_{10} = 6.1 \times 10^{10} \text{ M}^{-1}\text{s}^{-1}$ is derived. This rate constant presumably presents the first reduction step of the multicharged Au complex. It should be noted that depending on conditions, the formation of $\text{MV}^{\bullet+}$ in the presence of the metal complexes is followed by partial decay. As a result, partial decay of absorbance is observed, which is considerably slower than the build up. Corrections have been made for the relatively small contribution of this decay to the observed rate.

Reaction of $e_{\text{TiO}_2}^-$ with AuCl_4^- . The reduction of AuCl_4^- by $e_{\text{TiO}_2}^-$ (reaction 11) was studied by pulse radiolysis of deaerated solutions containing 0.2 M TiO_2 colloid in the presence of 0.5 M $(\text{CH}_3)_3\text{COH}$ at pH 2.6 and 1.5 μs pulse producing about 6×10^{-6} molar e_{aq}^- . Under these conditions most of the primary reducing radicals produced by the pulse react with the TiO_2 to

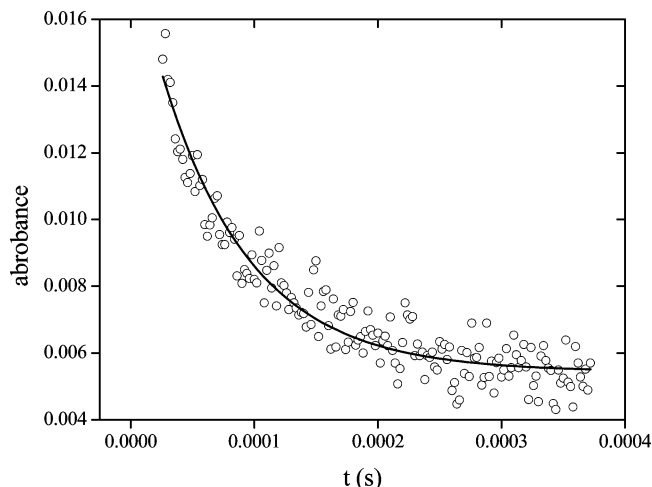


Figure 2. Decay of $e_{\text{TiO}_2}^-$ absorbance at 600 nm in the presence of HAuCl_4 after pulse radiolysis of argon-saturated solution containing 0.2 M TiO_2 , 6.3×10^{-6} M HAuCl_4 , 0.5 M $(\text{CH}_3)_3\text{COH}$ at pH 2.6. The line represents first-order rate law.

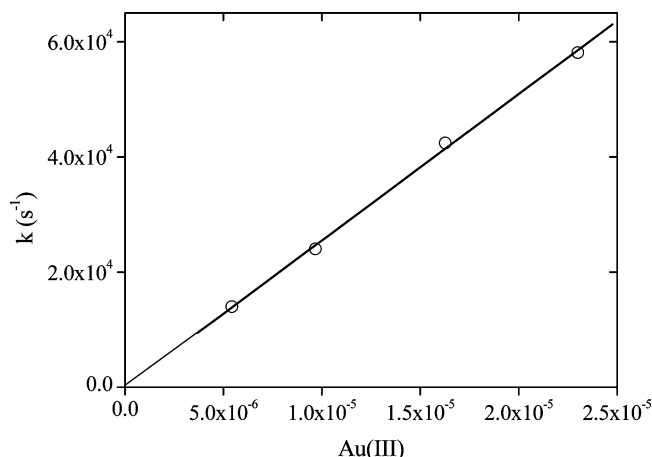
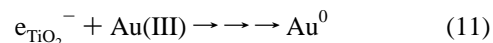


Figure 3. Pseudo first-order rate constant of reaction 11 as a function of $[\text{HAuCl}_4]$, 0.2 M TiO_2 , 0.5 M *tert*-butyl alcohol at pH 2.6, Ar-saturated.

form $e_{\text{TiO}_2}^-$. About 4–10% of these radicals may react with the gold complex,²⁵ depending on the gold concentration and competing with the studied reaction 11. Note that reaction 11 does not produce metallic gold directly, but the one and two electrons reduced metal complex intermediates disproportionate and regenerate in part the AuCl_4^- .



A typical example of the $e_{\text{TiO}_2}^-$ absorption decay at 600 nm is shown in Figure 2. The pseudo first-order rate constants for $e_{\text{TiO}_2}^-$ decay plotted versus AuCl_4^- concentration is given in Figure 3, from which $k_{11} = 2.5 \times 10^9 \text{ M}^{-1}\text{s}^{-1}$ is derived. In this plot the concentrations of AuCl_4^- have been corrected for the average depletion during reaction.

It should be noted that the rate constant derived here is about 3 orders of magnitude larger than the value of 2.5×10^6 measured for the parallel reaction of $e_{\text{TiO}_2}^-$ with H_2PtCl_6 .²²

Reduction of H^+ by $e_{\text{TiO}_2}^-$ in the Presence of TiO_2 Doped with Pd^0 , Pt^0 , and Au^0 . In a previous work²² we showed that the typical blue color of colloidal $e_{\text{TiO}_2}^-$ in acid solution, which is stable under argon for many days, disappears within several

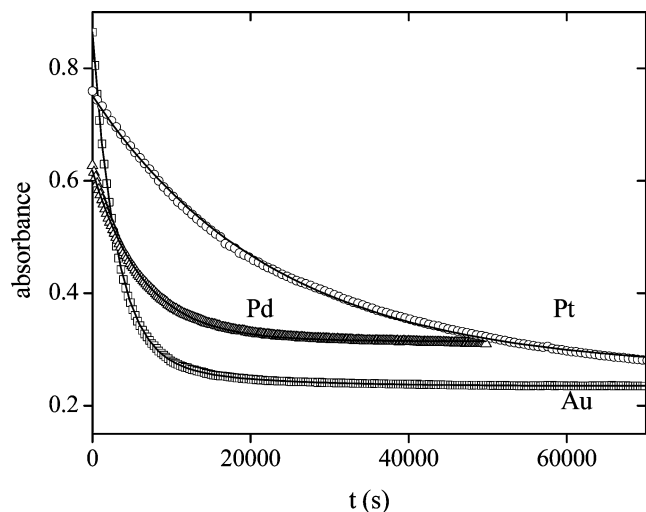


Figure 4. Effect of metal coatings on the rate of reaction 12. Absorbance induced by 30–40 pulses (total 900–1200 Gy) in 0.2 M TiO₂ Ar-saturated, in the presence of 0.2 M 2-propanol at pH 2.9. TiO₂ particles coated with $(1.3 \pm 0.1) \times 10^{-4}$ M Au⁰, Pd⁰ or Pt⁰. The solid lines represent first-order fits with the calculated pseudo rate constants, $k_{Au} = 3.4 \times 10^{-4} \text{ s}^{-1}$, $k_{Pd} = 1.8 \times 10^{-4} \text{ s}^{-1}$, and $k_{Pt} = 4.4 \times 10^{-5} \text{ s}^{-1}$.

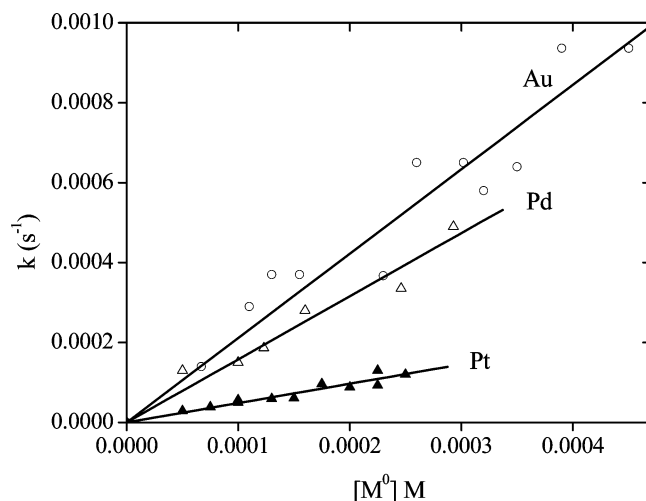
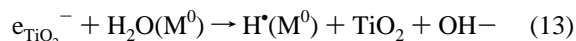
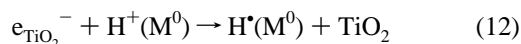


Figure 5. Effect of coating metal concentrations on the rate of reaction 12. The pseudo rate constants were taken from plots such as in Figure 4. 0.2 M TiO₂, 0.2 M 2-propanol at pH 2.6, Ar-saturated. The slopes of the straight lines correspond to $k_{Pt} = 0.48 \pm 0.02$, $k_{Pd} = 1.58 \pm 0.04$, and $k_{Au} = 2.1 \pm 0.1 \text{ s}^{-1}$.

hours when the TiO₂ is coated with Pt⁰ due to the reaction of $e_{TiO_2}^-$ with H⁺ and H₂O.



In the present work the decay kinetics of $e_{TiO_2}^-$ in TiO₂ coated with three different metals, Pt⁰, Pd⁰, and Au⁰, is compared (Figure 4). All three cases obey first-order rate law.

Kinetic measurements at different metal concentrations show linear dependency of $e_{TiO_2}^-$ decay rate with M⁰ concentration (Figure 5), resulting from increasing the number of active sites rather than the surface area of the adsorbed metals. In the latter case, $2/3$ power dependence on the metal concentration would be observed instead of the linear dependence. In contrast with the linear dependence reported here, Xu et al.²⁰ observed that increasing the amount of palladium deposition predominantly

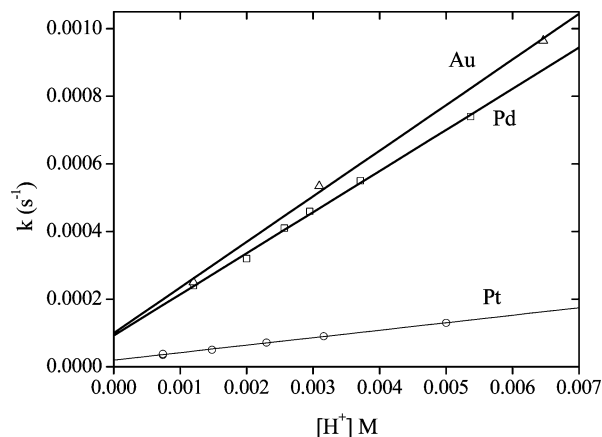
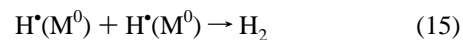
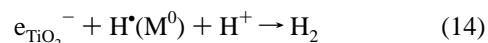


Figure 6. Effect of H⁺ concentration on the rate of reaction 12. Ar-saturated solutions of TiO₂ coated with 2×10^{-4} M Pd⁰, Au⁰, or Pt⁰. The rate constant calculated from plots such as in Figure 4. [TiO₂] = 0.2 M, 0.2 M 2-propanol. The slopes of the straight lines represent the pseudo first-order rate constant for reduction of H⁺: $k_{Pt}(H^+) = 0.022 \pm 0.004$, $k_{Pd}(H^+) = 0.12 \pm 0.01$, and $k_{Au}(H^+) = 0.14 \pm 0.01 \text{ s}^{-1}$. The intercepts represent the pseudo first-order rate constant of water reduction: $(2.0 \pm 0.2) \times 10^{-5}$, $(9 \pm 1) \times 10^{-5}$ and $(1.0 \pm 0.2) \times 10^{-4} \text{ s}^{-1}$, respectively.

induces growth of the initially formed seeds, and only a small portion of the metal form new seeds. This contradiction is attributed to different preparation methods of the clusters. Although Xu et al.²⁰ used sputtering of the Pd metal on TiO₂ surfaces, in the present work $e_{TiO_2}^-$ radicals were distributed randomly on the TiO₂ colloid particles before injecting the metal complex.

At a given metal M⁰ concentration the decay rate of $e_{TiO_2}^-$ increased linearly with H⁺ concentration for all metals tested as shown in Figure 6. This dependence means that hydrogen is produced predominantly by reaction 12 and to a much lesser extent by reaction 13 as can be concluded from the relatively small intercepts in Figure 6.

The adsorbed hydrogen radicals from reactions 12 and 13 produce molecular hydrogen by reactions 14 and 15. However, gold also catalyzes the reaction of H[•](M⁰) with 2-propanol; this will be discussed later.



Third-order rate constants for reaction 12, calculated from Figure 6 for the three metals are $k_{Pt} = 1 \times 10^2 [Pt^0] \text{ M}^{-1} \text{ s}^{-1}$, $k_{Pd} = 6 \times 10^2 [Pd^0] \text{ M}^{-1} \text{ s}^{-1}$, and $k_{Au} = 7 \times 10^2 [Au^0] \text{ M}^{-1} \text{ s}^{-1}$. These values are in fair agreement with those calculated from the results of Figure 5.

The TiO₂ used here has an average diameter of 5 nm and an average of 2000 TiO₂ molecules per particle. At the lowest [M⁰], the TiO₂ concentration in terms of colloid particles (each containing an average of 2000 TiO₂ molecules) is comparable to the atomic concentrations of the metals. Because the metal atoms tend to aggregate,²² most TiO₂ nanoparticles are not expected to have metal deposit. However, under our conditions $e_{TiO_2}^-$ builds up to a level of 10 excess electrons per TiO₂ particle. Under such conditions, if M⁰ interacts only with $e_{TiO_2}^-$ on the same nanoparticles, then a partial decay of these electrons is expected. This is in contradiction to the observed single-exponential decay accounting for most $e_{TiO_2}^-$ absorbance. The results indicate that $e_{TiO_2}^-$ produced on metal-free TiO₂ nanocrystallites decays by interparticle reaction involving metal

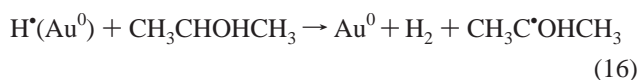
TABLE 1: Comparison of Hydrogen Yields of Different Doped Metals on TiO₂

metal	pH	$G(\text{H}_2)$ [M ⁰]0.1 mM	$G(\text{H}_2)$ [M ⁰]0.2 mM	$G(\text{H}_2)$ [M ⁰]0.2 mM
		0.2 M 2-PrOH	0.2 M 2-PrOH	2 M 2-PrOH
	2.6	2.4	2.38	2.4
Pd	2.6	4.5	*	4.3
Pt	2.6	4.8	4.75	4.8
Au	2.6	5.3	5.4	6.65

*Partial coagulation appeared before the GC measurement.

loaded nanocrystallites. Alternatively, the catalyst M⁰ may migrate from one nanocrystallite to another through the aqueous suspension between nanoparticles. Both colloid collision rate and equilibration between metal atoms in the bulk with metal aggregates on the TiO₂ nanosurfaces are much faster than the hour-long reduction of H⁺ to molecular hydrogen.

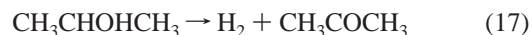
GC measurements. Yields of molecular hydrogen produced by reactions 1, 3, 14, and 15 have been determined after irradiating TiO₂ solutions in the presence as well as in the absence of the reduced metals. Measurements were carried out in argon-saturated 0.2–2 M (CH₃)₂CHOH at pH 2.6. Argon-saturated solutions containing only (CH₃)₂CHOH were used as a reference. In the reference solution the H₂ originates from three sources: (i) Reaction of e_{aq}[−] ($G = 2.7$) with H⁺ producing H[•] and subsequent dehydrogenation according to reaction 3. (ii) Primary H[•] atoms ($G = 0.6$) reacting according to (3). (iii) Molecular yield of H₂ ($G = 0.45$). The total yield sums up to $G = 3.75$. The evolution of H₂ in TiO₂ solutions in the absence of the reduced metals is expected to be lower because of competition between H⁺ and TiO₂ for the e_{aq}[−]. Taking the rate constant of e_{aq}[−] with H⁺ as $2.2 \times 10^{10} \text{ M}^{-1} \text{ s}^{-1}$ ²⁵ and e_{aq}[−] with TiO₂ as $2.6 \times 10^8 \text{ M}^{-1} \text{ s}^{-1}$,²⁴ 51% of the solvated electrons react with H⁺ at pH 2.6 to produce H₂ ($G = 1.4$). The rest of the solvated electrons produce e_{TiO₂}[−], which in the absence of M⁰ do not produce H₂. Because under these conditions practically all H atoms produce H₂ according to reaction 3, the calculated yield of H₂ is $1.4 + 0.45 + 0.6 = 2.45$. The average result from a large number of solutions is $G = 2.4 \pm 0.3$, in very good agreement with the calculated value. When M⁰ is also present, the H₂ yield is expected to increase to 5.4 (an erroneous value of 4.7 was reported previously)²² due to reactions (12–15). In fact, the hydrogen yield in the Pt⁰ and Pd⁰ systems is somewhat lower (Table 1). Presumably about 25% of the e_{TiO₂}[−] does not contribute to the formation of molecular hydrogen. This observation may be associated with trapped electrons, the reactions of which are too slow to be detected within the time of the measurements. Au⁰ induces the formation of higher yields compared to Pt⁰ and Pd⁰. Thus, with Au⁰/TiO₂ in 0.2 M 2-propanol the molecular hydrogen yield is 5.4, increasing to 6.65 at 2 M 2-propanol (Table 1). The effect of 2-propanol concentration is unique to the gold and is not observed in the other metal systems. The increased yield above $G(\text{H}_2) = 5.4$ is attributed to hydrogen abstraction from 2-propanol by H[•](Au⁰), according to reaction 16.



This abstraction induces a chain reaction because the 2-propanol radical produced by the hydrogen abstraction reacts with the nanoparticles according to reaction 6, thus regenerating the TiO₂ electron. The fact that $G(\text{H}_2)$ is only moderately increased compared to the Pt⁰ and Pd⁰ systems implies a relatively short chain, apparently due to the slowness of the hydrogen abstraction

reaction, which has to compete with reaction 15. The value $G(\text{H}_2) = 5.4$ in 0.2 M 2-propanol is determined by two opposite effects: The relatively slow trapped e_{TiO₂}[−] reaction discussed above, which decreases the observed hydrogen yield within the time of the measurement, and the above chain reaction.

Energy Balance. At pH 2.6 the redox potential of the titanium dioxide conduction band electrons is $\epsilon(\text{TiO}_2/\text{e}_{\text{TiO}_2}^-) = -0.12 - 0.059 \text{ pH} = -0.273 \text{ V}$,²⁶ compared to -1.39 V for the CH₃C[•]OHCH₃ free radical.²⁷ Although the metal layer may induce a negative shift,²⁸ in view of the large difference, conversion of e_{TiO₂}[−] to CH₃C[•]OHCH₃ is thermodynamically not feasible, unless simultaneous electron injection from the 2-propanol radical to the gold-coated TiO₂ (reaction 6) takes place. The net result of reactions 12, 16, and 6 is the material balance eq 17, the standard free energy of which is -6.11 kcal ²⁹ corresponding to $\epsilon = 0.1325 - 0.059 \text{ pH} = -0.0217 \text{ V}$ at pH 2.6. Thus, under the conditions of the above hypothesis the chain reaction sequence becomes thermodynamically feasible, provided that the energy of the surface TiO₂ electron and H[•](M⁰) does not differ much from that of the conduction band electron.



Note that although the rate constant of reaction 6 is considerably lower than the diffusion-controlled limit,²¹ the CH₃C[•]OHCH₃ radical is produced at the gold surface and is possibly linked to it. In such a case, nearly simultaneous reactions 16 and 6 become possible. The above suggestions are evidently speculative; however, we were unable to advance an alternative mechanism for the unexpectedly higher hydrogen yields in the gold system. The proposed chain reaction is in contradiction with Hussein and Rudham²³ who reported that Au/TiO₂ exhibit no activity for the photochemical dehydrogenation of 2-propanol. Our results on the hydrogen yields in the Au/TiO₂ system, compared to Pt/TiO₂ as given in the table are in discrepancy with the results of Bamwenda.¹⁷ In our work part of the total hydrogen yield ($0.45 + 1.35 + 0.6 = 2.4$) originates from the radiation products that do not involve e_{TiO₂}[−]; the rest of the measured yield, which originates from TiO₂ electrons, show the superiority of the gold over the platinum as catalyst in the H₂ production. This result is compared to the results of Bamwenda¹⁷ where the e_{TiO₂}[−] originates from photolysis of TiO₂ suspensions doped with Au⁰ and Pt⁰. The trend in the efficiencies of these two metals in our work is the opposite of their findings where the yield of H₂ production was about 30% lower than that obtained with Pt⁰. We do not have an explanation to this discrepancy. It may be possible that the discrepancy results from different properties of the doped TiO₂ particles because of different preparation procedures.

Conclusions

TiO₂ electrons were produced by electron injection of e_{aq}[−] and 2-propanol radicals via radiolysis of acid aqueous TiO₂ colloidal solutions. The e_{TiO₂}[−] decays within several hours when the TiO₂ nanoparticles were coated with Pd⁰, Pt⁰, or Au⁰. This decay is a result of catalyzed reaction between the e_{TiO₂}[−] and H⁺ to form H₂. The rate of decay is third order for all three metal systems, namely, first order in e_{TiO₂}[−], H⁺, and M⁰ concentrations. The decay rate of e_{TiO₂}[−] either as a function of [H⁺] at constant [M⁰] or as function of [M⁰] at constant [H⁺] is in the order Au⁰/TiO₂ > Pd⁰/TiO₂ > Pt⁰/TiO₂. The catalytic reduction gives rise to adsorbed hydrogen atoms, which combine to molecular hydrogen. Comparison of the measured H₂, produced upon irradiation, to the theoretical expected yield,

shows that about 25% of $e_{\text{TiO}_2}^-$ are trapped and do not contribute to molecular hydrogen during the time of the measurement. The catalytic efficiency of the doped metals is in the order $\text{Au}^0/\text{TiO}_2 > \text{Pt}^0/\text{TiO}_2 \geq \text{Pd}^0/\text{TiO}_2$, with Pt^0 and Pd^0 having almost the same yield with a difference that is in the range of the measurement accuracy. The Au^0/TiO_2 has a higher yield attributed to a short chain reaction involving hydrogen abstraction from 2-propanol by the adsorbed H atom, followed by electron injection to the TiO_2/Au particle from the adsorbed 2-propanol radical.

Acknowledgment. We express our gratitude to Eran Gilead for maintenance of the electron beam system and to Yair Ozery for assistance with gas chromatography measurements.

References and Notes

- (1) Bard, A. J. *J. Phys. Chem.* **1982**, *86*, 172.
- (2) Baba, R.; Nakabayashi, S.; Fujishima, A.; Honda, K. *J. Phys. Chem. B* **1985**, *89*, 1902.
- (3) Heller, A. *Pure Appl. Chem.* **1986**, *58*, 1189.
- (4) Domen, K.; Sakata, Y.; Kudo, A.; Maruya, K.; Onishi, T. *Bull. Chem. Soc. Jpn.* **1988**, *61*, 359.
- (5) Anpo, M.; Chiba, K.; Tomonari, M.; Coluccia, S.; Che, M.; Fox, M. A. *Bull. Chem. Soc. Jpn.* **1991**, *64*, 543.
- (6) Bard, A. J.; Fox, M. A. *Acc. Chem. Res.* **1995**, *28*, 141.
- (7) Li, F. B.; Li, X. Z. *Chemosphere* **2002**, *48*, 1103.
- (8) Bahnemann, D. W.; Hilgendorff, M.; Memming, R. *J. Phys. Chem. B* **1997**, *101*, 4265.
- (9) Graetzel, M. *Heterogeneous Photochemical Electron Transfer*; CRC Press: Boca Raton, FL, 1989.
- (10) Wang, C. M.; Heller, A.; Gerischer, H. *J. Am. Chem. Soc.* **1992**, *114*, 5230.
- (11) Subramanian, V.; Wolf, E. E.; Kamat, P. V. *J. Am. Chem. Soc.* **2004**, *126*, 4943.
- (12) Wood, A.; Giersig, M.; Mulvaney, P. *J. Phys. Chem. B* **2001**, *105*, 8810.
- (13) Chiang, K.; Lim, T. M.; Tsen, L.; Lee, C. C. *Appl. Catal., A* **2004**, *261*, 225.
- (14) Crittenden, J. C.; Liu, J. B.; Hand, D. W.; Perram, D. L. *Water Res.* **1997**, *31*, 429.
- (15) Choi, W.; Lee, J.; Kim, S.; Hwang, S.; Lee, M. C.; Lee, T. K. *J. Ind. Eng. Chem.* **2003**, *9*, 96.
- (16) Einaga, H.; Harada, M.; Futamura, S.; Ibusuki, T. *J. Phys. Chem. B* **2003**, *107*, 9290.
- (17) Bamwenda, G. R.; Tsubota, S.; Nakamura, T.; Haruta, M. *J. Photochem. Photobiol., A* **1995**, *89*, 177.
- (18) Kiwi, J.; Graetzel, M. *J. Phys. Chem.* **1984**, *88*, 1302.
- (19) Kanno, H.; Yamamoto, Y.; Harada, H. *Chem. Phys. Lett.* **1985**, *121*, 245.
- (20) Xu, C.; Lai, X.; Zajac, G. W.; Goodman, D. W. *Phys. Rev. B* **1997**, *56*, 13464.
- (21) Gao, R. M.; Safrany, A.; Rabani, J. *Radiat. Phys. Chem.* **2003**, *67*, 25.
- (22) Kasarevic-Popovic, Z.; Behar, D.; Rabani, J. *J. Phys. Chem. B* **2004**, *108*, 20291.
- (23) Hussein, F. H.; Rudham, R. *J. Chem. Soc., Faraday Trans. 1* **1987**, 2817.
- (24) Gao, R. M.; Safrany, A.; Rabani, J. *Radiat. Phys. Chem.* **2002**, *65*, 599.
- (25) Neta, P.; Huie, R.; Ross, A. B. *J. Phys. Chem. Ref. Data* **1988**, *17*, 1027.
- (26) Nozik, A. J. *Annu. Rev. Phys. Chem.* **1978**, *29*, 189.
- (27) Schwarz, H. A.; Dodson, R. W. *J. Phys. Chem.* **1989**, *93*, 409.
- (28) Schmelling, D. C.; Gray, K. A.; Kamat, P. V. *Environ. Sci. Technol.* **1996**, *30*, 2547.
- (29) Clark, W. M. *Oxidation Reduction Potentials of Organic Systems*; Robert E. Krieger Publishing Company: Huntington, NY, 1972.